RSC Advances

This is an *Accepted Manuscript*, which has been through the Royal Society of Chemistry peer review process and has been accepted for publication.

Accepted Manuscripts are published online shortly after acceptance, before technical editing, formatting and proof reading. Using this free service, authors can make their results available to the community, in citable form, before we publish the edited article. This *Accepted Manuscript* will be replaced by the edited, formatted and paginated article as soon as this is available.

You can find more information about *Accepted Manuscripts* in the Information for Authors.

Please note that technical editing may introduce minor changes to the text and/or graphics, which may alter content. The journal's standard Terms & Conditions and the Ethical guidelines still apply. In no event shall the Royal Society of Chemistry be held responsible for any errors or omissions in this *Accepted Manuscript* or any consequences arising from the use of any information it contains.

ROYAL SOCIETY OF CHEMISTRY

www.rsc.org/advances

RSC Advances

RSCPublishing

Paper

Silver-Coordination Polymer Network Combining Antibacterial Action and Shape Memory Capability

Cite this: DOI: 10.1039/x0xx00000x

Received 00th January 2012,
Accepted 00th January 2012

DOI: 10.1039/x0xx00000x

www.rsc.org/

Lin Wang, Wenxi Wang, Shubin Di, Xifeng Yang, Hongmei Chen, Tao Gong, and Shaobing Zhou*

In this study, a multifunctional polymer network is achieved by, first, isonicotinate-functionalized polyesters (PIE) is synthesized via classical melt-condensation polymerization, second, the pendant of the pyrazinamide groups on the polyester side chains is coordinated with Ag ions to form the physically cross-linking network. The thermo property analysis and the dynamic mechanical analysis display that the Ag-coordination polymer network possesses an excellent thermo-induced shape memory function both under the air condition and the physiological condition due to a widely glass transition temperature region. The Ag ion concentration coordinated with polymer was optimized to achieve the best shape memory effect with Atomic Absorption Spectrometry. Moreover, the coordinated polyester can act as a reservoir of bactericidal Ag ions, in which Ag ions are released measured with Inductively Coupled Plasma Mass Spectrometry, and in turn the antibacterial function is realized. Finally, the result of Alamar blue assay reveals that the Ag coordinated polyester has good cytocompatibility in spite of the introduction of a certain of Ag ions. Therefore, the multifunctional polymer has greatly potential application in the biomedical field, e.g., burn wound dresssings.

Introduction

Shape memory polymers (SMPs) as a class of stimuli-sensitive materials that could memorize a temporary shape and recover their initial shape in response to an environmental stimulus.[1-3] To date, SMPs have been widely investigated for their great potential applications in biomedical device, especially the thermo-induced SMPs.[4-5] These polymers can be deformed into a compact form or other forms according to the need of surgery and in turn the shape memory function probably allows them to be delivered both conveniently and safely, subsequently recover to complex final shapes in vivo upon exposure to the body temperature.[6] Generally, SMPs consist of fixity phase for recover their initial shape and reversible phase for formation and fixation of the temporary shape.[7] The fixity phase is either chemical cross-linking or physical cross-linking structure. Generally, the chemical cross-linking structure contain the active chemical groups such as diisocyanate and cinnamon groups,[8-9] and the physical cross-linking structure contain the entanglement of molecular chains or the hydrogen bonding.[10-13] Most recently, a metal–ligand coordination has been utilized to form a new physical cross-linking structure in obtaining shape memory hydrogel. For example, Liu reported a shape memory hydrogel with an imidazole–zinc ion coordination [14] and triple-shape memory poly (acrylonitrile 2-methacryloyloxyethyl phosphorylcholine) based on the Dipole–Dipole-Zinc Ion coordination.[15] In contrast to the chemical cross-linking or physical cross-linking structure previously reported, the formation of the metal–ligand coordination is simple and the condition is mild. The metal–ligand coordination polymers are compounds containing the

RSC Advances Accepted Manuscript

coordinative interaction of metal ions and the charged or neutral organic ligands.[16-17] The ligands mainly include N-donor ligands. Among these ligands, reactive pendant isonicotinic acid group is widely used as a kind of pyridinium-type ligands.[18] Silver ion is considered as an ideal candidate to form coordination polymers. In addition, it has one of the highest levels of toxicity for microorganisms, yet the least toxicity for eukaryotic cells.[19] Ag is used in many cases for disinfection, and polymer complexes with Ag ion have great potential for applications in medical instruments.[20-24] Moreover, the mechanism of antibacterial action and clinical toxicology have been reviewed systematically.[25-27]

In this study, our concept for implementing a combination of the antibacterial action and the shape memory capability is a silver-coordination polymer network. This network is fabricated on the basis of Ag-coordinated isonicotinate-functionalized polyester (PIE) (Ag-PIE), in which pyrazinamide groups located in polymer side chain provide a ligand effect. Low toxicity of isonicotinic acid has been verified by previous research.[28] Since the Ag-coordinated polyester has a physical cross-linking structure, it displays good shape memory function. Simultaneously, the polymer network is endowed with an antibacterial property due to the introduction of Ag ions. The coordinated polyester can act as a reservoir of bactericidal Ag ions, in which they are released, and in turn the antibacterial function will be realized.

Experimental Section

Materials

isonicotinic acid, sebacic acid, diethanolamine (DEA) were purchased from Kelong chemical reagent factory in Chengdu (China). Sebacic acid were recrystallized before use. And the other chemical reagents were of reagent grade and used without further purification. The cells belonged to normal cell line, which were from neonatal rat's mandibular. They have been passaged to the third generation just before our experiments. The Escgerichia coli (E.coli, ATCC 25922) was selected for the antibacterial experiment.

Preparation of N,N-Bis (2-hydroxyethyl) pyrazinamide (BIN).

BIN was synthesized through an ammonolysis reaction from methyl isonicotinate and DEA as shown in Sch. 1A. Firstly, methyl isonicotinate was synthesized from isonicotinic acid and methanol under H_2SO_4 as catalyst in 60 ℃ for 4 h, after it was finished and cooled to room temperature, $NaHCO_3$ solution was added into the reaction liquid into neutral, and then methyl isonicotinate was extracted from solution by methylene chloride. After that, BIN was synthesized from methyl isonicotinate and DEA under Ar at 90 ℃ for 24 h. Lastly, BIN was obtained by extract from deionized water/crude product. And the white solid was obtained.

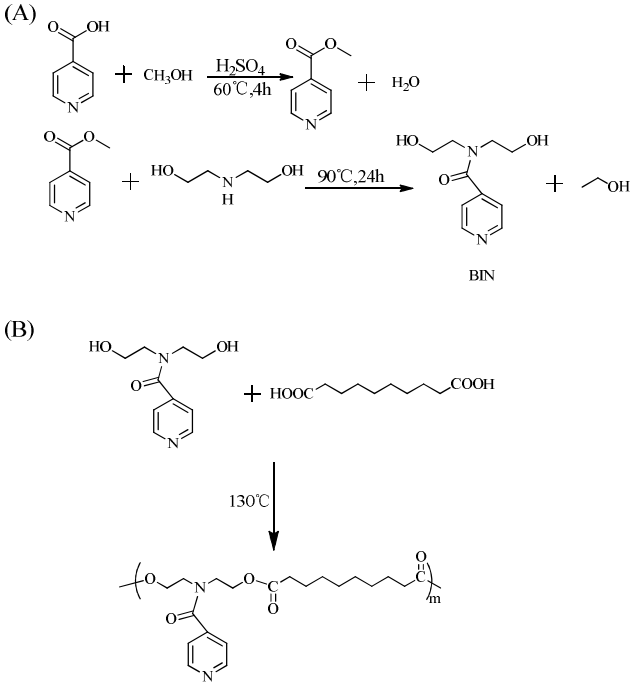

Sch.1 Synthetic route of BIN(A) and PIE.

Preparation of isonicotinate-functionalized polyesters (PIE). The PIE was synthesized through melt phase polycondensation as shown in Sch. 1B. Briefly, 10 mmol BIN and 10 mmol sebacic acid were combined by melting at 130 ℃ under a blanket of Ar. Then the polycondensation reaction under the reduced pressure for 24 h. A transparent light yellow viscous product was obtained. After the reaction, the viscous product was poured into PTFE mold and the PIE film could obtained when it cooled. And the molecular weight of PIE measured by GPC, and the molecular weight is 45200, and the polydispersity is 1.467.

Preparation of Ag-PIE.

Firstly, polymer was soaked into 4 g/L $AgNO_3$ solution for 1 h, then wiped the water of surface and further dried under vacuum at room temperature for 24 h, finally, the Ag-PIE films were prepared for DMA, shape memory test, antibacterial performance test.

The absorption of Ag ions.

The Ag-PIE samples were immersed in 20 mL 4 g/L $AgNO_3$ solution for 1 h, and the $AgNO_3$ solution at the designated time were analyzed with Atomic Absorption Spectrometry (AAS, Thermo Elemental S4).

Ag ions release.

The Ag ion release from the Ag-PIE was measured with Inductively Coupled Plasma Mass Spectrometry (ICP, NexION 300X). The Ag-

RSC Advances Accepted Manuscript

This journal is © The Royal Society of Chemistry 2012

PIE samples were immersed in 10 mL of phosphate buffer solution (PBS) in 25 ℃ and 37 ℃ for 24 h. And when the Ag-PIE samples were immersed in PBS for 2 h, 4, 8, 16, 24, 30 h, 2 mL PBS was pipetted at each time point. Then the PBS solutions containing the released Ag ions at the designed time were measured by ICP.

Characterisation.

FT-IR was measured by Nicolet 5700 IR spectrometer. All samples were obtained by KBr plates in which dry power was mixed with KBr at a weight ratio of 0.5-1%. ^{1}H-NMR spectra were obtained on a Bruker AM-300 spectrometer. Tetramethylsilane (TMS) was used as the internal standard and $CDCl_3$ was used as solvent. Thermal properties of polymers were determined by DSC (TA DSC-Q100). In order to eliminate any unknown thermal history of the samples, heating and cooling were repeated from −20 ℃ to 120 ℃, the DSC curves of the second heating and cooling process were obtained. Both the heating and cooling ratio was 10 ℃/min. All data were used from the second heating process. DMA was measured using a specimen with size of 10 × 3 × 1 mm (length × width × thickness) carried out with a DMA (TA DMA-Q 800) at heating ratio of 3 ℃ /min from 0 to 80 ℃ and at frequency of 1 Hz. The storage modulus E' and tan datle were tested. Gel permeation chromatography (GPC) was performed with a Water 2695 separation module equipped with a StyragelHT4DMF column calibrated with polystyrene narrow standards operated at 40% and series 2414 refractive index detector.

Investigation of the thermo-induced shape memory effect.

The thermo-induced shape memory properties were measured using strip specimens of the Ag-PIE. The strip was heated at 50 ℃ for 1 min so that they could be softened, and was bended to a spiral shape, named as temporary shape. Then, the deformed specimen was moved to a 0 ℃ ice water for freezing stress and fixing deformed shape for 1 min. When the spiral shape specimen was induced with 40 ℃ hot air, it could be observed that it could recovery to its initial shape.

Shape memory fixity ratio and recovery ratio were measured using strip shaped specimens measured by DMA with a controlled force mode according to our designed experiment. A typical testing procedure was performed as previous report.[29] Firstly, straining the specimen at a constant stress rate at 45 ℃ obtained a temporary shape, marked as ε_1 ; and then cooled to 0 ℃ and released the stress, marked as ε_2; Secondly, the temporary shape was heated from 0℃ to 45 ℃, the strain marked as ε_0. The shape memory fixity ratio and recovery ratio were calculated according to the following equations:

$$R_f = \frac{\varepsilon_2}{\varepsilon_1} \times 100\% \quad (1)$$

$$R_r = \left(1 - \frac{\varepsilon_0}{\varepsilon_1}\right) \times 100\% \quad (2)$$

Antibacterial performance assay.

The escherichia coli (ATCC 25922) was selected in the antibacterial experiment. Each specimen was sterilized through UV light for 24h before the experiment. The antibacterial performance assays was evaluated based on the two methods, coating method and Alamar blue assay as previous report.[30] The bacteria were cultivated in a beef extract-peptone (BEP) medium (GB/T 4789.28) at 37℃ for 12 h, and then 1 mL of bacterial suspension was taken out and dispersed into 9 mL of PBS until the concentration of bacterial suspension was adjusted to approximately 10^5 colonyforming units (CFU/mL). Each sample was put in 5 mL of the bacterial suspension in the dark at 37 ℃ for 5 h. then 100 μL of each bacterial suspension was taken out and spread onto a nutrient agar plate and 10 mL medium/PBS, respectively, then the specimen added into the plate and the fluid culture medium, after that the samples incubated at 37 ℃ for 24 h. Finally, through the appearance of bacteriostatic ring and the Alamar blue assay to investigate the antibacterial performance. A sample of 200 μL of reduced Alamar blue solution was pipetted into a costar opaque black bottom 96-well plate (Sigma) and read at 600 (emission) in an ELISA microplate reader (Molecular Devices, Sunnyvale, CA).

In vitro cytotoxicity assays.

The cytotoxicity assays was evaluated based on the Alamar blue assay as our previous report. [31] In brief, all the samples were cut into small round flakes at an average diameter of nearly 12 mm to be used for osteoblasts culture in vitro. After that the osteoblasts were grown in RPMI medium 1640 (Gibcos) with 10% fetal bovine serum (FBS). These cells with a density of 1×10^4 cells/well were cultured in 24-well plate (Sigma) in the above medium and maintained at 37 ℃ in a humidified incubator with 5% CO_2. At the predesigned time points of 1, 3, 5 days, the medium was removed and 300 μL Alamar blue solution (10% Alamar blue, 80% media 199 (Gibcos) and 10% FBS; v/v) was added into each well and incubated for further 3 h. Blank controls were wells without materials. A sample of 200 μL of reduced Alamar blue solution was pipetted into a costar opaque black bottom 96-well plate (Sigma) and read at 570 (excitation) / 600 (emission) in an ELISA microplate reader (Molecular Devices, Sunnyvale, CA). Cell morphology and growth on the PIE films were

RSC Advances Accepted Manuscript

evaluated by fluorescence microscopy (DMIL, Leica, Germany) and all cells were stained by calcein.

Results and discussion

The isonicotinate-functionalized polyesters (PIE) was synthesized via classical melt-condensation polymerization under high vacuum at 130 ℃. The composition of the polyester and Ag-coordinated polyester were investigated using Fourier transform infrared spectroscopy (FT-IR) and Proton nuclear magnetic resonance (^{1}H-NMR). Fig. S1 in the Support Information (SI) shows the FT-IR spectra of the N, N-Bis (2-hydroxyethyl) pyrazinamide (BIN) and the PIE, the ^{1}H-NMR of the BIN. In the FTIR spectrum of the BIN as shown in Figure S1A, it exhibits characteristic absorptions of C-N stretching vibration at 1470 cm^{-1} and the N-C=O stretching vibration at 1620 cm^{-1}. In the ^{1}H-NMR of the BIN (Fig. S1B), the chemical shifts at 3.15 ppm, 3.61 ppm, 7.81 ppm and 8.89 ppm are attributed to –N-CH_2-, -CH_2-OH and pyridine H atoms, respectively. From the FT-IR spectra of the PIE and Ag-PIE in Fig. S2, we can clearly find that the PIE exhibits characteristic absorptions of C-N stretching vibration at 1450 and 1490 cm^{-1}, while the red shift occurs in the FTIR spectrum of Ag-PIE due to the ligand coordinating with Ag ion, indicating that the coordination polymer has been synthesized successfully. And from the results of Figure S3 in SI, we could observe that there is an obvious difference in transmittance. In the UV-vis curve of Ag-PIE, there is a maximum transmissive peak at 410 nm, is owing to the Ag

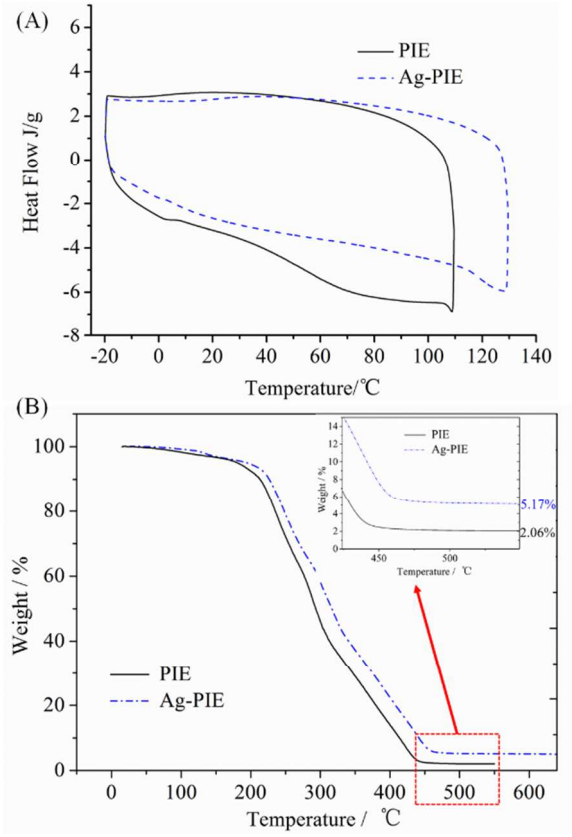

Fig. 1 DSC (A) and TG (B) curve of PIE and Ag-PIE.

Ions. The changes of PIE and Ag-PIE from the results of FTIR and UV-vis indicate that the coordination polymer was prepared successfully.

The thermal transition temperatures of the PIE and Ag-PIE were investigated by Differential scanning calorimetry (DSC) analysis using the second heating thermogram. It can be observed from Fig. 1A that all specimens shows a wide glass transition temperature region from 20 ℃ to ~80 ℃. To verify the amount of adsorbed Ag ions, Thermogravimetric (TG) analysis was carried out as shown in Fig.1B. The TG curve of PIE shows a weight loss of 98% from 0 ℃ to 500 ℃ for the decomposition of PIE, however, for the Ag-PIE, the temperature of decomposition increases, suggesting that the polyester coordinated with Ag ion have a better stability. From the weight loss, the amount of adsorbed Ag ions in this polymer network could be calculated and its concentration is about 3.11%.

The dynamic mechanical behavior depending on temperature is an important factor for the investigation of SMPs because it could predict the shape memory properties and provide information for shape fixity and recovery.[32] Fig. 2 shows the storage modulus and tan delta curves of the PIE and Ag-PIE. When at lower temperature,

RSC Advances Accepted Manuscript

This journal is © The Royal Society of Chemistry 2012

the Ag-PIE has a higher storage modulus (1130 MPa) than that (950 MPa) of initial polymer. A high glassy-state modulus

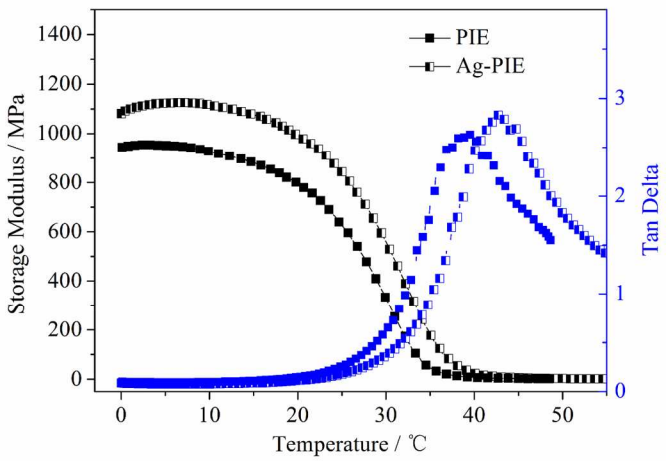

Fig. 2 DMA curves of the PIE and the Ag-PIE.

would provide the material with a good shape fixity when cooling, yet a high rubbery modulus could lead to a large elastic recovery at high temperature,[33] and this theory is a basic condition of the shape memory polymers.[34] Based on those guidelines, we can infer that the Ag-PIE possesses an excellent shape memory effect. And from the result of tan delta, we can find that the Ag-PIE has a higher transition temperature from20 ℃ to 55 ℃ than the transition temperature of the PIE, which is consistent with the result of DSC analysis. The wide glass transition temperature region could provide the deformed and recovery temperature of the shape memory process.

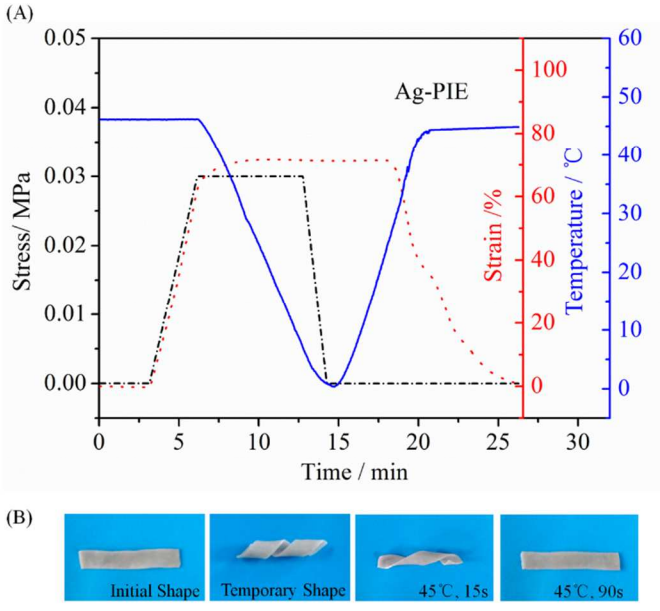

Fig. 3 Shape memory properties of Ag-PIE measured by DMA (A); shape memory fixing and recover process (B).

Thermo-induced shape memory effect of the Ag-PIE was further investigated by Dynamic mechanical analysis (DMA) with a controlled force mode. The quantitative demonstration of thermo-induced shape memory properties of the Ag-PIE is shown in Fig. 3A. In the stress-strain-temperature curves, the Ag-PIE exhibits an excellent shape memory effect, and the shape fixity ratio and recovery ratio remain above 95% calculated from the equations (1) and (2). Moreover, from the shape memory fixity and recovery process of Ag-PIE (Fig. 3B), also we can see that the Ag-PIE exhibit good shape fixity ratio and shape recovery ratio. All samples were repeated three times, and both the shape fixity ratio and recovery ratio remain more than 95%.

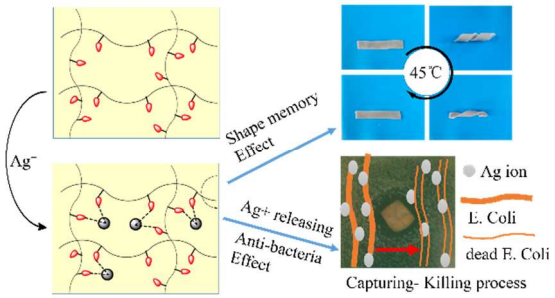

Sch. 1 The mechanisms of shape memory and the antibacterial effect of the Ag-PIE.

The proposed thermo-induced shape memory mechanism for the Ag-PIE is shown in Sch. 1. In this shape memory system, the pyrazinamide groups introduced into the polymer side chain provide the ligands. Later, after the PIE is immersed in $AgNO_3$ solution, with the solution penetrating into polymer matrix the ligands of PIE can easily coordinate with Ag ions to form a physical cross-linking structure. In the process of shape memory, the physical cross-linking structure can act as the fixity phase to provide the elasticity for recovering their initial shape. The polyester molecular chains acts as the reversible phase for the formation and fixation of the temporary shape.

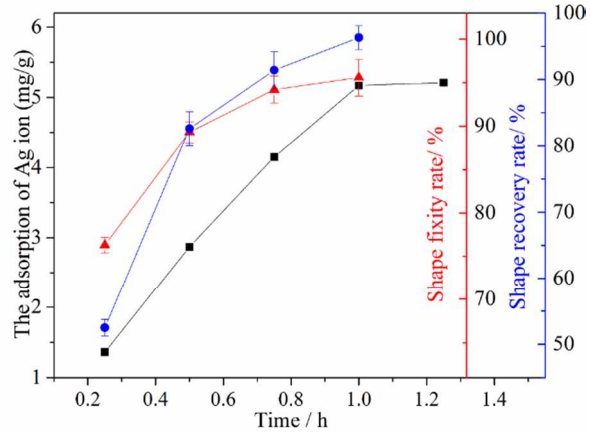

RSC Advances Accepted Manuscript

Fig. 4 Shape fixity and shape recovery ratio under different amount of absorbed Ag ions.

The Ag ions concentration coordinated with polymer was further optimized to achieve the best shape memory effect. The absorption of Ag ions was measured by Atomic Absorption Spectrometry (AAS, Thermo Elemental S4). At 22 ℃, the Ag-PIE film samples were firstly immersed in 20 mL 4 g/L $AgNO_3$ solution for 15 min, 30 min, 45 min, 60 min, 75 min, respectively. Then the accumulated amount of absorbed Ag ions at the designated time was analyzed with AAS. In Fig. 4, it can be observed that with the increase of immersion time, the amount of absorbed Ag ions increases to about 5 mg/g (Ag ion/PIE) until 60 min. After that, the amount of Ag inos almost maintains unchangeable. Therfore, the Ag-PIE immersed for 60 min was selected for all investigations.

The effect of the amount of the absorbed Ag ions on shape memory property was investigated. In Figure 4, the shape fixity rate and the shape recovery rate increase with the increasing of absorbed Ag ions, which is also due to the increasing of the cross-linking effect from the coordination with Ag ions. When the amount of absorbed Ag ions reached about 5 mg/g obtained from AAS analysis, the maximum shape fixity and recovery rate could be achieved.

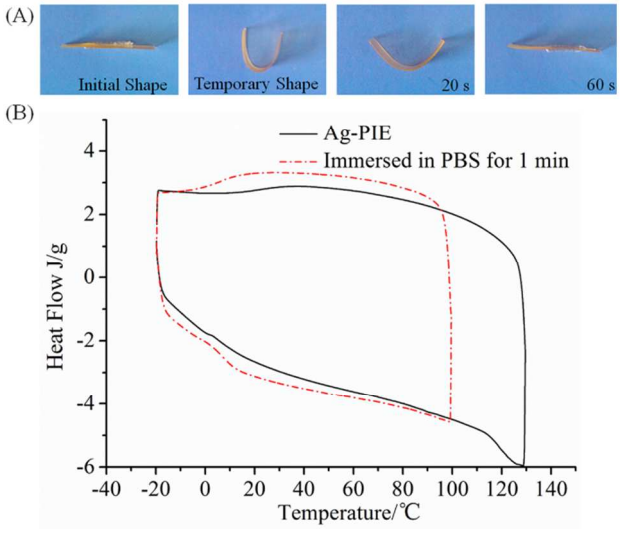

Fig. 5 Shape memory effect of Ag-PIE in PBS at 37 ℃ (A); DSC curves of Ag-PIE before and after immersed in PBS for 1 min (B).

Additionally, as a potential biomedical material, the investigation of shape memory effect upon to physiological conditions is necessary. The shape memory process in phosphate buffer solution (PBS) at 37 ℃ for Ag-PIE is shown in Fig. 5A. It can be found that the Ag-PIE also possess a good shape memory property, and it can recovery its initial shape in 60 s. Fig. 5B shows the DSC curves of Ag-PIE and the sample immersed in PBS for 1 min and the results indicate that there is a pronounced decrease in transition temperature after immersed in PBS for 1 min due to the absorption of water. The faster recovery of the immersed sample can be ascribed to the decrease of the transition temperature.

For medical devices, the antibacterial function is very vital for their implanting in vivo in resisting bacterial infection. The antibacterial property of the Ag-PIE was investigated. Firstly, the release of Ag ions from the Ag-PIE respectively at 25 ℃ for storage and 37 ℃ for in vivo application were studied using Inductively Coupled Plasma Mass Spectrometry (ICP, NexION 300X). In Fig. 6A, the concentrations of the released Ag ions at 25 ℃ could reach 0.61 ppm after 24 h, while the concentrations of the released Ag ions at 37 ℃ were 0.18 ppm after 2 h and up to 0.91 ppm after 24 h. The Ag ions can damage bacterial cell membrane thus alter its function, but its cytotoxicity to normal cell cannot be ignored. The maximum Ag ion concentration has been reported to be less than 10 mg/L.[35] In our study, the accumulated release amount of Ag ions both at 25 and 37 ℃ is much less than 10 mg/L, so we think that the Ag-PIE can be potentially applied as biomaterial.

RSC Advances Accepted Manuscript

This journal is © The Royal Society of Chemistry 2012

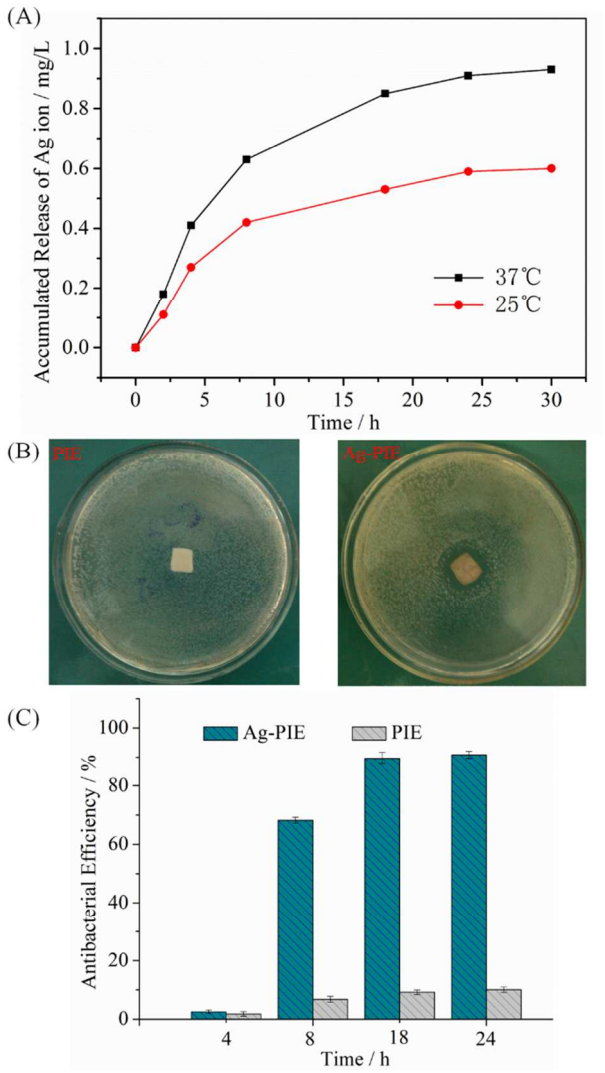

Fig. 6 Ag ion release profiles in PBS at 37 ℃ and 25 ℃, respectively (A); Bacterial colonies of PIE and Ag-PIE (B) and the antibacterial efficiency of Ag-PIE compared with PIE against E.coli (C)

Fig. 6B shows the antibacterial effect of the Ag-PIE against escherichia coli. The PIE without the Ag coordination could not bring any effect on the bacterial growth, while the Ag-PIE had obvious antibacterial activity. Figure 6C shows the antibacterial activity of the samples against escherichia coli in the fluid culture medium at 37 ℃. We can find that the Ag-PIE has an antibacterial efficiency of 92% after 24 h. The proposed antibacterial shape memory mechanism for the Ag-PIE is shown in Scheme 1. Ag ions could be released from the coordinated polyester to provide the antibacterial effect.

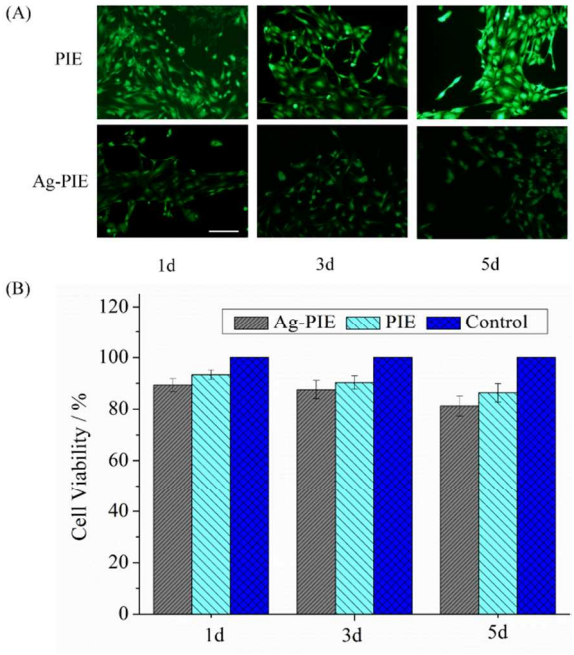

Fig. 7 Cell viability (A) and Fluorescence images (B) showing the osteoblasts cultured on the PIE and Ag-PIE substrates at day 1, 3, and day 5, respectively. Cells were strained by calcein and all the scale bars represent 25 μm.

The excellent non-cytotoxicity is an important characteristic of biomaterials. So *in vitro* cytotoxicity of the PIE and the Ag-PIE was further assessed by measuring the viability of osteoblast cells with Alamar blue assay. From Fig. 7A, it can be observed that the cell viability remained greater than 85 % for all specimens, moreover, the viability in the Ag-PIE group was not significantly different from that of the cells cultured on PIE. This result indicates that the PIE coordinated with a certain amount of Ag ions still can keep good cytocompatibility. The morphology of osteoblasts is observed by fluorescence microscopy after being stained by calcein as shown in Fig. 7B. It can be clearly found that the osteoblasts grew healthily and attached well on the all films. It also demonstrated that the released Ag ions in the scope of the security. Therefore, the Ag-coordination polymer network combining the antibacterial action and shape memory capability is potentially suitable for the applications in medicine.

Conclusion

In summary, we originally developed one type of silver-coordination polymer network combining the excellent shape memory function and the highly antibacterial action via a simple strategy. In this polymer network, the pyrazinamide groups located in polymer side chains provide a ligand effect with the absorbed Ag ions to endow the shape memory function, and the coordinated polyester acts as a

RSC Advances Accepted Manuscript

reservoir of Ag ions to allow them be gradually released. By quantitatively optimizing the Ag ion amount in polymer network, the good balance was achieved among the antibacterial action, shape memory function and cytocompatibility. The multifunctional polymer has great potential for the application as smart medical device.

Acknowledgements

This work was partially supported by National Basic Research Program of China (973 Program, 2012CB933600), National Natural Science Foundation of China (No.30970723 and No.51173150), Research fund for the Doctoral Program of Higher Education of China (20120184110029) and Construction Program for Innovative Research Team of University in Sichuan Province (14TD0050).

Notes and references

Key Laboratory of Advanced Technologies of Materials, Ministry of Education, School of Materials Science and Engineering, Southwest Jiaotong University, Chengdu, Sichuan 610031, PR China

E-mail: Shaobingzhou@hotmail.com; shaobingzhou@swjtu.edu.cn

Electronic Supplementary Information (ESI) available: [details of any supplementary information available should be included here]. See DOI: 10.1039/b000000x/

1. A. Lendlein, S. Kelch, *Angewandte Chemie International Edition,* 2002**,** *41*, 2034.
2. M. Behl, A. Lendlein, *Mater. Today* **2007,** *10*, 20.
3. H. Xu, C. Yu, S. Wang, V. Malyarchuk, T. Xie, J. A. Rogers, *Adv. Funct. Mater.* **2013**, *23*, 3299.
4. A. Beilvert, F. Chaubet, L. Chaunier, S. Guilois, G. Pavon-Djavid, D. Letourneur, A. Meddahi-Pellé, D. Lourdin, *Carbohyd Polym.* **2014**, *99*, 242.
5. K. Kratz, U. Voigt, A. Lendlein, *Adv. Funct. Mater.* **2012**, *22*, 3057.
6. X. Liu, K. Zhao, T. Gong, J. Song, C. Bao, E. Luo, J. Weng, S. Zhou, *Biomacromolecules* **2014**, *15*, 1019.
7. J. Leng, X. Lan, Y. Liu, S. Du, *Prog. Mater. Sci.* **2011**, *56*, 1077.
8. Shao, C. Lavigueur, X. X. Zhu, *Macromolecules* **2012**, *45*, 1924.
9. L. Wang, X. Yang, H. Chen, T. Gong, W. Li, G. Yang, S. Zhou, *ACS Appl. Mater. Inter.* **2013**, *5*, 10520.
10. W. Voit, T. Ware, R. R. Dasari, P. Smith, L. Danz, D. Simon, S. Barlow, S. R. Marder, K. Gall, *Adv Funct Mater* **2010**, *20*, 162.
11. X. Zheng, S. Zhou, X. Li, J. Weng, *Biomaterials* **2006**, *27*, 4288.
12. D. J. Davies, A. R. Vaccaro, S. M. Morris, N. Herzer, A. P. Schenning, C. W. Bastiaansen, *Adv. Funct. Mater.* **2013**, 23, 2723.
13. S. Zhou, X. Zheng, X. Yu, J. Wang, J. Weng, X. Li, B. Feng, M. Yin, *Chem. Mater.* **2007**, *19*, 247.
14. W. Nan, W. Wang, H. Gao, W. Liu, *Soft Matter* **2013**, *9*, 132.
15. Y. Han, T. Bai, Y. Liu, X. Zhai, W. Liu, *Macromol. Rapid. Comm.* **2012**, *33*, 225.
16. J. R. Kumpfer, S. J. Rowan, *J. Am. Chem. Soc.* **2011**, *133*, 12866.
17. I. Chevrier, J. L. Sagué, P. S. Brunetto, N. Khanna, Z. Rajacic, K. M. Fromm, *Dalton T.* **2013**, *42*, 217.
18. A. Muñoz-Bonilla, M. Fernández-García, *Prog. Polym. Sci.* **2012**, *37*, 281
19. S. Chernousova, M. Epple, *Angew. Chem. Int. Edit.* **2013**, *52*, 1636.
20. K. M. Fromm, *Appl. Organomet Chem.* **2013**, *27,* 683.
21. K. Wang, Y. Yin, C. Li, Z. Geng, Z. Wang, *CrystEng. Comm.* **2011**, *13*, 6231.
22. V. W. L. Ng, J. P. K. Tan, J. Leong, Z. X. Voo, J. L. Hedrick, Y. Y. Yang, *Macromolecules* **2014**, *47*, 1285.
23. P. K. Fyfe, V. A. Rao, A. Zemla, S. Cameron, W. N. Hunter, *Angew. Chem. Int. Edit*. **2009**, *121*, 9340.
24. A. Agarwal, K. M. Guthrie, C. J. Czuprynski, M. J. Schurr, J. F. McAnulty, C. J. Murphy, N. L. Abbott, *Adv. Funct. Mater.* **2011**, *21*, 1863.
25. J. S. Lee, W. L. Murphy, *Adv. Mater.* **2013**, *25*, 1173.
26. J. Maillard, P. Hartemann, *Crit. Rev. Microbiol.* **2013**, *39*, 373.
27. A. Alonso, X. Muñoz Berbel, N. Vigués, R. Rodríguez Rodríguez, J. Macanás, M. Muñoz, J. Mas, D. N. Muraviev, *Adv. Funct. Mater.* **2013**, *23*, 2450.
28. E. Torres, E. Moreno, S. Ancizu, C. Barea, S. Galiano, I. Aldana, A. Monge, S. Pérez-Silanes, *Bioorg. Med. Chem. Lett.* **2011**, *21,* 3699
29. C. Liu , H. Qin , P. T. Mather, *J. Mater. Chem.* **2007**, 17, 1543.
30. D. Ratna, J. Karger-Kocsis, *J. Mater. Sci.* **2008**, *43*, 254.
31. Y. Liu, K. Gall, M. L. Dunn, P. McCluskey, *Mech. Mater.***2004**, *36*, 929.
32. A. Roguska, M. Pisarek, M. Andrzejczuk, M. Lewandowska, K. J. Kurzydlowski, M. Janik Czachor, *J. Biomed. Mater. Research.* **2012**, *100*, 1954.
33. C. H. Kim, E. J. Choi, J. K. Park, *J. Appl. Polym. Sci*. **2000**, *77*, 2049.
34. C. Zhao, B. Feng, Y. Li, J. Tan, X. Lu, J. Weng, *Appl. Surf. Sci*. **2013**, 280, 8.
35. S. Shao, S. Zhou, L. Li, J. Li, C. Luo, J. Wang, X. Li, J. Weng, *Biomaterials* **2011**, *32*, 2821.

RSC Advances Accepted Manuscript

 This journal is © The Royal Society of Chemistry 2012

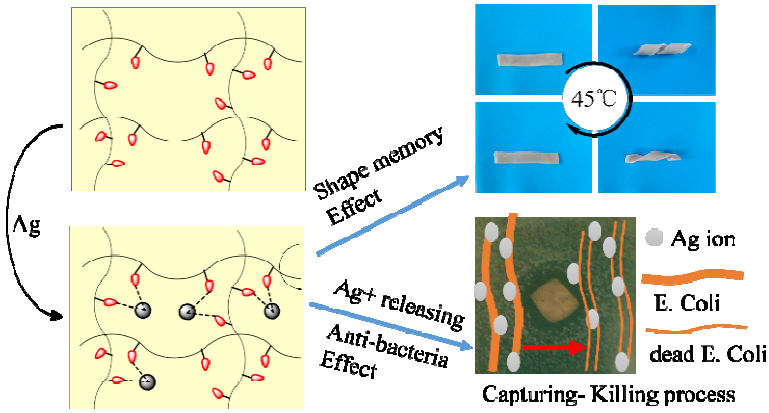

Ag-coordination polymer network displays a shape memory function and simultaneously allows Ag ions be released to exert an antibacterial activity.

RSC Advances Accepted Manuscript